Application Note
Stem Cell Research

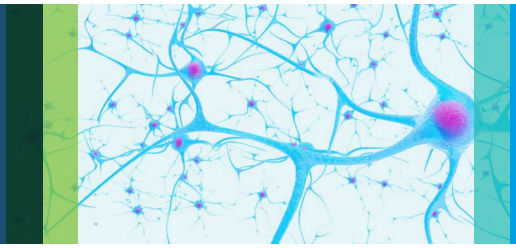

Agilent
Trusted Answers

Glycolytic Suppression - The Impact of Metabolic Modulation on Neural Stem Cell Fate

Authors

Kanwaldeep Singh*,
McMaster University,
Hamilton, Ontario, Canada

Ned Jastromb,
Agilent Technologies, Inc.
Cell Analysis Division,
Lexington, MA USA

Yoonseok Kam,
Agilent Technologies, Inc.
Cell Analysis Division,
Lexington, MA USA

George W. Rogers
Agilent Technologies, Inc.
Cell Analysis Division,
La Jolla, CA USA

Abstract

Cellular metabolism is emerging as a critical factor in stem cell research with recent reports suggesting that both metabolic status and cell culture conditions can significantly alter the differentiation trajectory of stem cells. *In vitro* metabolic profiling provides information to identify key metabolic changes associated with stem cell differentiation. Agilent Seahorse XF technology enables real-time measurement of glycolytic and mitochondrial function along the cell differentiation axis. By changing the metabolic environment in the design of differentiation experiments, metabolic profiling can be incorporated to probe cell function, and more importantly, to guide improved differentiation outcomes. Here, an assay design is introduced for sequential metabolic profiling during induced pluripotent stem cell (iPSC) differentiation toward neural progenitor cells (NPCs) using human skin fibroblast-derived iPSCs, singularized and cultured *in vitro*. Results suggest that metabolic modulation during stem cell differentiation can affect stem cell specification, as well as the final differentiated cell yield and quality. This design can be applied to better understand the interrelationship between metabolic poise and differentiation, thus enabling the development of improved differentiation protocols.

Introduction

Human induced pluripotent stem cells (iPSCs) provide an ideal platform for patient-specific disease modeling and regenerative therapies. These cells offer an unlimited patient-specific stem cell source with the potential for differentiation into unique cell types within the body[1]. Neuronal lineages are extensively explored for both disease modeling and regenerative therapeutics purposes[2-6]. A critical and transitionary step in the process of neuronal lineage formation is derivation of NPCs which have the capacity to proliferate and differentiate into most neuronal cell types within the human body. Current studies have started to decipher the molecular and metabolic checkpoints that occur during iPSC differentiation into neurons[7-10], yet, protocols to induce iPSC differentiation towards an NPC phenotype can be inefficient and yield low numbers of cells[11-15].

**with guidance from Dr. Eva Szabo's Laboratory*

Recently, the use of alternative carbon sources to drive specific metabolic pathways that initiate lineage specification has been investigated[16-18]. For example, switching glucose to galactose as an alternative carbon source in the culture media results in the promotion of oxidative phosphorylation and hence, differentiation-specific pathways which ultimately direct cell fate decisions[19]. Here, the metabolic drivers for specification by use of alternative carbon sources are evaluated for the neuronal lineage by measuring both mitochondrial and glycolytic function with the Agilent Seahorse XF Cell Mito Stress Test and the Agilent Seahorse XF Glycolytic Rate Assay, respectively. Results indicate that altering the carbon source from glucose to galactose promotes switching from a glycolytic to an oxidative phosphorylation phenotype that is correlated to improved NPC differentiation from human iPSCs.

Results

Experimental design of metabolic rate measurements using singularized iPSCs *in vitro*

iPSCs derived from human skin fibroblasts were singularized to facilitate tracking of the changes in metabolic phenotype, as well as the expression of molecular markers for iPSCs and NPCs. As briefly summarized in Figure 1 and detailed in the Materials and Methods section, iPSCs were singularized and transferred to Agilent Seahorse XF96 Cell Culture Microplates and differentiated for 10 days towards NPC phenotype by sequential media changes within the XF96 plates and on conventional 12-well plates, for XF analysis and immunostaining,

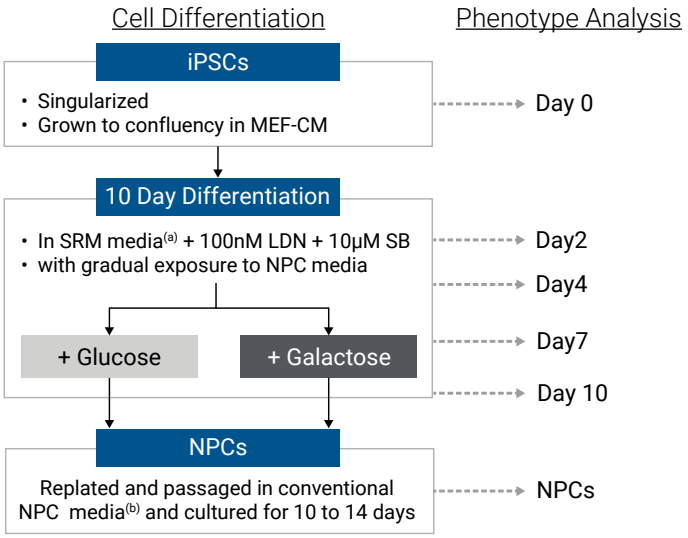

Figure 1. Schematic of the iPSC differentiation to NPC workflow, protocol, and phenotypic measurement time points. The metabolic profile and differentiation status were monitored at the indicated time points using Agilent Seahorse XF analysis and immunofluorescence staining during the differentiation process.

respectively. The singularized and monolayer-cultured iPSCs showed stable expression of the stem cell markers Oct4 and Nanog, similar to the parental colonies (Figure 2).

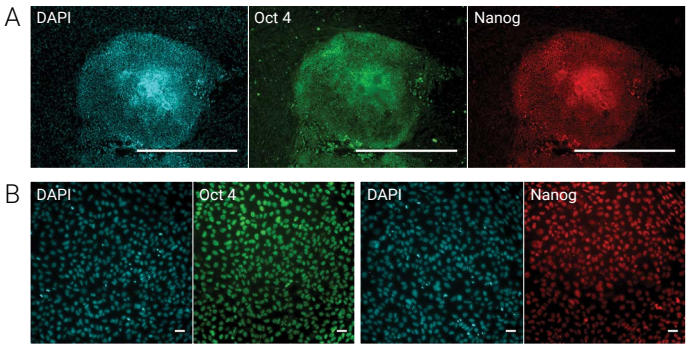

Figure 2. iPSCs in 2D culture express pluripotency markers. Representative images show expression of pluripotency markers, Oct4 and Nanog in parental iPSC colonies (A) and singularized iPSCs (B). Scale bar = 100 µm.

Replacement of glucose with galactose promotes iPSC differentiation to an NPC phenotype

It has been well established that when the major carbon source of glucose is replaced with galactose, glycolytic energy metabolism is suppressed while mitochondrial respiration remains intact[19]. Interestingly, the NPC population obtained after performance of the complete iPCS differentiation to NPC workflow/protocol (Figure 1) showed different metabolic activities depending on the carbon source supplemented during differentiation. As shown in Figures 3A-D, NPCs obtained from galactose differentiation conditions showed overall lower metabolic function when compared to Day 0 iPSCs. Metabolic parameters of basal OCR, spare respiratory capacity (SRC), basal PER and compensatory glycolysis all decreased in the presence of galactose when compared to the NPC cells obtained with glucose, which maintained a metabolic phenotype similar to the original iPSCs. Further, galactose containing media increased the Nestin-positive cells in the NPC population obtained after differentiation, indicating increased efficiency of the differentiation process (Figure 3E). In summary, this suggests that while galactose reduces metabolic activity as measured by OCR and PER, it causes an increased reliance on aerobic metabolism, and promotes faster, more efficient differentiation, as measured by Nestin expression.

Modulation of iPSC culture conditions influences iPSC differentiation quality

The improvement of differentiation quality when substituting the iPSC media with galactose was evident several days after the induction, and could be detected earlier than NPC marker expression. In the presence of galactose, the NPC differentiation appeared to be more homogeneous, with a gradual appearance of Nestin (+) cells (Figure 4A). A significant majority of the iPSCs appeared to be differentiated into Nestin (+) cells by day 10, whereas in the presence of glucose, the differentiation was heterogeneous and less

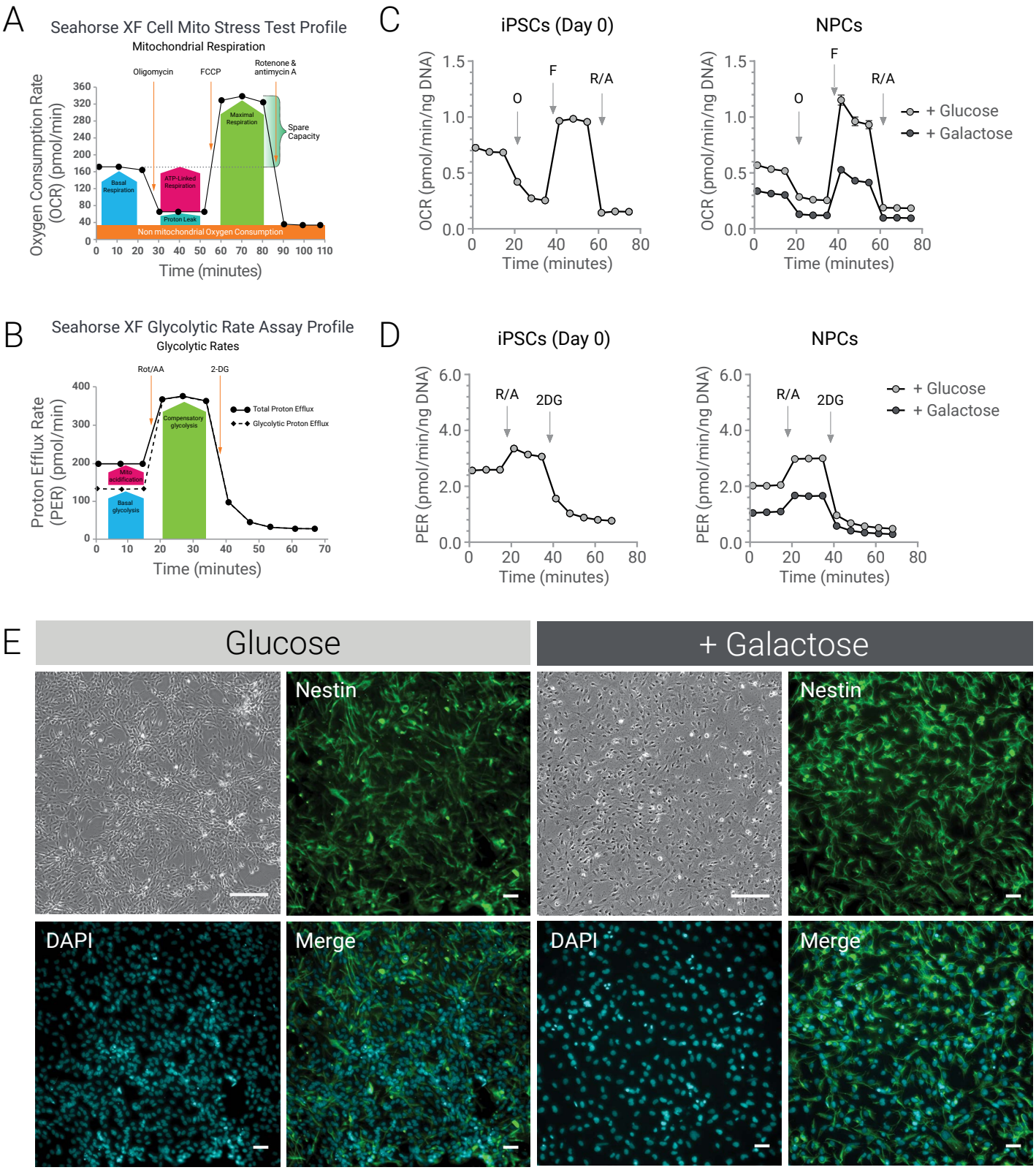

Figure 3. Metabolic function and NPC marker expression are altered by the change in carbon source. Mitochondrial and glycolytic function of iPSCs (Day 0) and resulting NPCs in the presence of glucose or galactose (Figure 1) were compared by using the Seahorse XF Cell Mito Stress Test (A, C) and Glycolytic Rate Assay (B, D). Error bars reported as mean ± S.E.M. (n = 60 for iPSCs and 20 for NPCs). (E) NPC differentiation was confirmed by immunofluorescence staining of the NPC marker, Nestin. Scale bar = 100 µm.

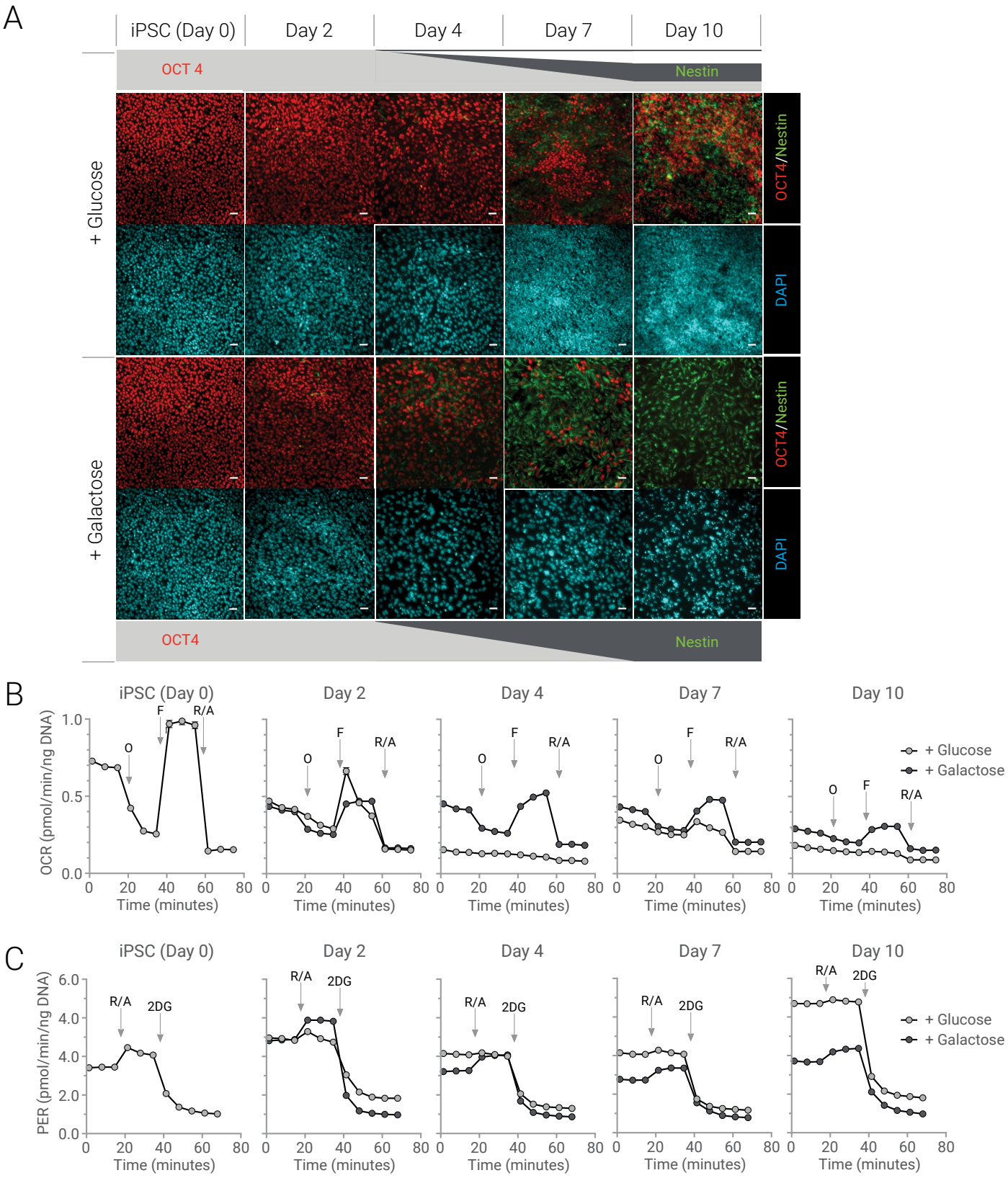

Figure 4. Carbon source change affects metabolic reprograming and the quality of differentiation from iPSCs to NPCs. Representative immunofluorescence images stained for the pluripotency marker, Oct4 and the NPC marker, Nestin at the indicated time points during differentiation in either glucose- or galactose-containing media (A). Scale bar = 100 µm. Mitochondrial respiration (B) and glycolysis (C) were traced from day 0 to day 10 of the iPCS differentiation to NPC workflow as described in Figure 1 and Materials and Methods. Error bars reported as mean ± S.E.M. (n=24 from Day 2 to Day 10 and n=60 for iPSCs).

efficient, as a significant proportion of Oct4(+) and Oct4(-)/Nestin(-) cells were still present at day 10 in the differentiation timeline (Figure 4A). Differences were also identified in metabolic functional changes (Figures 4B-C and Figure 5). In the presence of galactose, cells showed more sustained mitochondrial basal respiration and higher SRC throughout the differentiation process when compared to cells differentiated in the presence of glucose (Figure 4B and 5A-B). In contrast, mitochondrial respiration was significantly decreased in the presence of glucose, especially SRC and further, the cells showed higher basal glycolytic rates, with similar or slightly increased compensatory glycolysis (Figure 4C and 5C-D). These substantially different outcomes of the differentiation process in the presence of glucose or galactose as the main carbon source are summarized in Table 1, illustrating more rapid and efficient differentiation of iPSCs.

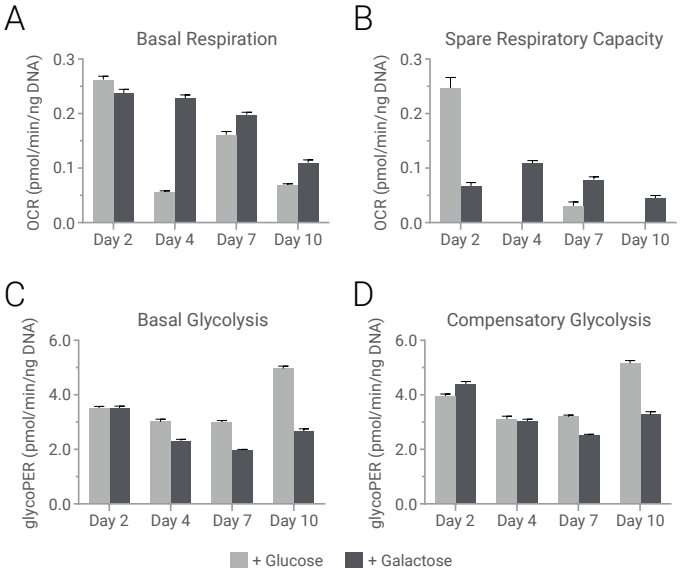

Figure 5. Differentiation-associated early metabolic phenotype transition is altered by a change in carbon source. Mitochondrial functional parameters (A, B) and glycolytic functional parameters (C, D) are compared. Significant differences were detected from day 4-10 between groups differentiated in the presence of glucose or galactose. Error bars reported as mean ± S.E.M. (n > 14).

Carbon Source		Glucose	Galactose
Cell yield on Day 10 of differentiation	Total (x10^6 cells)	8.44 ± 0.21	5.55 ± 0.21
	Viable (x10^6 cells)	2.37 ± 0.29	3.75 ± 0.22
	Viability (%)	28.0 ± 2.8	67.0 ± 3.5
NPC yield at the first passage	Total (x10^6 cells)	3.45 ± 0.14	16.47 ± 1.01
	Viable (x10^6 cells)	3.18 ± 0.18	15.30 ± 1.27 [a]
	Viability (%)	92.0 ± 0.7	92.0 ± 2.1
Time to the 1st NPC passage		18 days	4 days [b]
NPC Differentiation Efficiency		+	++++

(a) 4.8 fold increase in live NPC cell numbers obtained under Galactose condition vs. Glucose
(b) 4.5 fold increase in proliferation capacity of Day 10 populations when replated in NPC media

Table 1. The efficiency of iPSC to NPC differentiation was improved by differentiation media conditions that included galactose as a replacement for glucose as a carbon source.

Discussion

Metabolic analysis, surrogate pluripotency and early neural stem/progenitor cell marker expression were examined during the timeline of human iPSC differentiation towards an NPC. Analysis of glycolytic activity and mitochondrial respiration over the time course of differentiation demonstrated that under glucose conditions, basal respiration rates and spare respiratory capacity are significantly decreased. Further, glycolytic activity is significantly higher than that observed for galactose conditions. Conversely, under galactose conditions, basal respiration and spare respiratory capacity are maintained (albeit at decreasing rates) throughout the differentiation timeline, with a concomitant decrease in glycolytic function. The results in Table 1 illustrate that by replacing glucose with galactose during the early stage of differentiation (i.e. exit from pluripotency) the differentiation timeline was accelerated (4 vs. 18 days to first NPC passage) and the yield of NPCs improved approximately 5 fold, as measured by decreasing Oct4 expression and increasing Nestin expression.

With respect to metabolic function under galactose conditions, the decrease in glycolysis with maintenance of mitochondrial respiration during the differentiation process suggests that these forced metabolic conditions. Therefore, establishing NPC differentiation protocols that drive a metabolic transition from glycolysis to oxidative phosphorylation may enhance the formation of stable and more homogeneous NPC populations. These results underscore the power of real-time functional metabolic analysis, in conjunction with orthogonal data, to enable a better understanding of the role of metabolism during cellular differentiation, with the goal of developing more efficient and robust differentiation methods.

Conclusion

Metabolic profiling using the Seahorse XF Cell Mito Stress Test and Glycolytic Rate Assay to measure mitochondrial respiration and glycolysis can be used to analyze and pinpoint metabolic switches and mechanisms that affect iPSC differentiation with respect to speed and efficiency. Here, decreases in glycolysis and maintenance of mitochondrial respiration appear to be correlated with increased NPC differentiation efficiency from iPSCs. In general, these types of assays provide a robust means towards understanding the metabolic drivers of cell differentiation and thus predicting and programing cell fate specification toward an NPC (or other) terminal phenotype.

Materials and Methods

Cell culture

Human skin fibroblast-derived iPSCs derived were cultured in Mouse Embryonic Fibroblasts-Conditioned Media (MEF-CM) supplemented with 8 ng/mL bFGF (PeproTech, 100-18B) on culture dishes coated with Matrigel (Corning, 354234). NPCs derived from iPSCs were cultured on Matrigel-coated cell culture dishes in 10 mM glucose-supplemented NPC media; glucose-free DMEM (Thermo, 11966025), 1X N2 (Thermo, 17502048), 1X B27 (Thermo, 17504044), 10 ng/mL bFGF, and 50 ng/mL EGF (PeproTech, AF-100-15).

Differentiation of iPSCs into NPCs

For differentiation of iPSCs into NPCs, iPSCs were dissociated with Accutase (Corning, 25-058-CI) and filtered through a 0.45 µm filter to remove any remaining cell clumps. They were then resuspended in MEF-CM, supplemented with 10 µM Y-27632 (Abcam, ab144494) and 8 ng/mL bFGF, and plated on gelatin-coated cell culture dishes at 37 °C for 30 minutes to remove fibroblasts. Nonadherent cells were collected, counted, and plated at a density of 5.0×10^4 cells/cm^2 in MEF-CM supplemented with 10 µM Y-27632 and 8 ng/mL bFGF on Matrigel-coated cell culture plates with daily media changes until the cells reached confluency. Upon confluency, the neural differentiation was induced (day 0) in either 10 mM glucose (Sigma, G7021) or 10mM galactose (Sigma, G5388) supplemented differentiation media. This differentiation media composition is glucose-free DMEM with 15% KOSR (Knock-Out Serum Replacement; Thermo, 10828028), 1X NEAA (Non-essential amino acids; Thermo, 11140050), 1 mM sodium pyruvate (Thermo, 11360070), 100 nM LDN-193189 (Cayman Chemicals, 11802), and 10 µM SB-431542 (Cayman Chemicals, 13031). The media was refreshed daily until day 2. On day 4, media was replaced with the respective differentiation media mix with glucose- or galactose-containing NPC media at 3:1 ratio. The media mix rate was changed to 1:1 on day 6 and to 1:3 on day 8. On day 10, the cells were dissociated with Accutase and replated on Matrigel-coated cell culture dishes in 10 mM glucose-containing NPC media until cells reached confluency with media changes every other day.

Cellular metabolic profiling

Singularized iPSCs were plated and differentiated in Seahorse XF96 V3 PS Cell Culture Microplates (Agilent, 101085-004) plates as described previously. The metabolic data were measured on the days indicated in Figure 1 using both the Seahorse XF Cell Mito Stress Test Kit and the Seahorse XF Glycolytic Rate Assay. Both assays were performed in Seahorse XF DMEM without phenol red, pH 7.4 (Agilent 103575-100) supplemented with 2.5 mM L-Glutamine (Agilent, 103579-100), 1 mM sodium pyruvate (Agilent, 103578-100), and 10 mM glucose (Agilent, 103577-100). The optimal FCCP concentration (0.5 µM) was used for the XF Cell Mito Stress Test kit. Once iPSCs reached confluency, the mitochondrial and glycolytic metabolic profiles were measured before the induction of differentiation (day 0) data, this was followed by a series of assays on days after the onset of differentiation on the Seahorse XF96 plates as indicated in Figure 1 to track the metabolic changes during differentiation. To obtain the metabolic profiles of NPCs, cells were cultured for an additional 10-14 days in NPC culturing conditions after seeding at a density of 6×10^4 cells/well on Matrigel-coated Seahorse XF96 plates. XF Cell Mito Stress Test and XF Glycolytic Rate Assay measurements were performed on these cell using the Agilent Seahorse XFe96 Analyzer, and were normalized to cellular DNA content using the CyQuant Cell Proliferation assay kit (Thermo, C7026). All functional parameters were calculated using the XF Cell Mito Stress Test and XF Glycolytic Rate Assay report generators.

Immunofluorescence staining

iPSCs were plated in 12-well plates and differentiated as described previously. After 10 days of differentiation, cells were replated on Matrigel-coated 12-well plates in NPC media and grown until 70–80% confluency. iPSC colonies, NPCs, and the differentiating cells at specified time points during NPC differentiation were fixed using BD Cytofix/CytoPerm kit (BD Bioscience, 554714). Upon fixation, cells were blocked in 10% normal donkey serum (Millipore Sigma, S30-100ML) for 1 hour at room temperature. This was then followed by overnight incubation with primary unconjugated antibodies against Oct4 (Cell Signaling Technology, 2890S) and Nestin (Abcam, Ab22035) at 4 °C. The next day, cells were washed three times and stained with Alexa Fluor-488 (Thermo, A11029) and Alexa Fluor-647 (Thermo, A21245) conjugated secondary antibodies at room temperature for 1 hour. Cells were washed three times, stained with DAPI (Thermo, D3571), and then imaged.

References

1. Robinton, D. A.; Daley, G. Q., The promise of induced pluripotent stem cells in research and therapy. *Nature* **2012**, 481 (7381), 295–305.
2. Bordoni, M.; Rey, F.; Fantini, V.; Pansarasa, O.; Di Giulio, A. M.; Carelli, S.; Cereda, C., From Neuronal Differentiation of iPSCs to 3D Neuro-Organoids: Modelling and Therapy of Neurodegenerative Diseases. *International journal of molecular sciences* **2018**, 19 (12).
3. Brennand, K. J.; Simone, A.; Jou, J.; Gelboin-Burkhart, C.; Tran, N.; Sangar, S.; Li, Y.; Mu, Y.; Chen, G.; Yu, D.; McCarthy, S.; Sebat, J.; Gage, F. H., Modelling schizophrenia using human induced pluripotent stem cells. *Nature* **2011**, 473 (7346), 221-5.
4. Kaye, J. A.; Finkbeiner, S., Modeling Huntington's disease with induced pluripotent stem cells. *Molecular and cellular neurosciences* **2013**, 56, 50–64.
5. Lai, W. S.; el-Fakahany, E. E., Interaction of 4-aminopyridine with [3H]phencyclidine receptors in rat brain homogenates. *Neuroscience letters* **1986**, 67 (1), 87–91.
6. Li, L.; Chao, J.; Shi, Y., Modeling neurological diseases using iPSC-derived neural cells : iPSC modeling of neurological diseases. *Cell and tissue research* **2018**, 371 (1), 143–151.
7. Christie, K. J.; Emery, B.; Denham, M.; Bujalka, H.; Cate, H. S.; Turnley, A. M., Transcriptional regulation and specification of neural stem cells. *Advances in experimental medicine and biology* **2013**, 786, 129-55.
8. Lees, J. G.; Gardner, D. K.; Harvey, A. J., Mitochondrial and glycolytic remodeling during nascent neural differentiation of human pluripotent stem cells. *Development* **2018**, 145 (20).
9. O'Brien, L. C.; Keeney, P. M.; Bennett, J. P., Jr., Differentiation of Human Neural Stem Cells into Motor Neurons Stimulates Mitochondrial Biogenesis and Decreases Glycolytic Flux. *Stem cells and development* **2015**, 24 (17), 1984-94.
10. Zheng, X.; Boyer, L.; Jin, M.; Mertens, J.; Kim, Y.; Ma, L.; Ma, L.; Hamm, M.; Gage, F. H.; Hunter, T., Metabolic reprogramming during neuronal differentiation from aerobic glycolysis to neuronal oxidative phosphorylation. *eLife* **2016**, 5.
11. Cheng, C.; Fass, D. M.; Folz-Donahue, K.; MacDonald, M. E.; Haggarty, S. J., Highly Expandable Human iPS Cell-Derived Neural Progenitor Cells (NPC) and Neurons for Central Nervous System Disease Modeling and High-Throughput Screening. *Current protocols in human genetics* **2017**, 92, 21 8 1–21 8 21.
12. Hook, L.; Vives, J.; Fulton, N.; Leveridge, M.; Lingard, S.; Bootman, M. D.; Falk, A.; Pollard, S. M.; Allsopp, T. E.; Dalma-Weiszhausz, D.; Tsukamoto, A.; Uchida, N.; Gorba, T., Non-immortalized human neural stem (NS) cells as a scalable platform for cellular assays. *Neurochemistry international* **2011**, 59 (3), 432-44.
13. Kim, D. S.; Lee, D. R.; Kim, H. S.; Yoo, J. E.; Jung, S. J.; Lim, B. Y.; Jang, J.; Kang, H. C.; You, S.; Hwang, D. Y.; Leem, J. W.; Nam, T. S.; Cho, S. R.; Kim, D. W., Highly pure and expandable PSA-NCAM-positive neural precursors from human ESC and iPSC-derived neural rosettes. *PloS one* **2012**, 7 (7), e39715.
14. Koch, P.; Opitz, T.; Steinbeck, J. A.; Ladewig, J.; Brustle, O., A rosette-type, self-renewing human ES cell-derived neural stem cell with potential for in vitro instruction and synaptic integration. *Proceedings of the National Academy of Sciences of the United States of America* **2009**, 106 (9), 3225-30.
15. Nemati, S.; Hatami, M.; Kiani, S.; Hemmesi, K.; Gourabi, H.; Masoudi, N.; Alaei, S.; Baharvand, H., Long-term self-renewable feeder-free human induced pluripotent stem cell-derived neural progenitors. *Stem cells and development* **2011**, 20 (3), 503-14.
16. Correia, C.; Koshkin, A.; Duarte, P.; Hu, D.; Teixeira, A.; Domian, I.; Serra, M.; Alves, P. M., Distinct carbon sources affect structural and functional maturation of cardiomyocytes derived from human pluripotent stem cells. *Scientific reports* **2017**, 7 (1), 8590.
17. Marsboom, G.; Zhang, G. F.; Pohl-Avila, N.; Zhang, Y.; Yuan, Y.; Kang, H.; Hao, B.; Brunengraber, H.; Malik, A. B.; Rehman, J., Glutamine Metabolism Regulates the Pluripotency Transcription Factor OCT4. *Cell reports* **2016**, 16 (2), 323–332.
18. Tohyama, S.; Fujita, J.; Hishiki, T.; Matsuura, T.; Hattori, F.; Ohno, R.; Kanazawa, H.; Seki, T.; Nakajima, K.; Kishino, Y.; Okada, M.; Hirano, A.; Kuroda, T.; Yasuda, S.; Sato, Y.; Yuasa, S.; Sano, M.; Suematsu, M.; Fukuda, K., Glutamine Oxidation Is Indispensable for Survival of Human Pluripotent Stem Cells. *Cell metabolism* **2016**, 23 (4), 663-74.
19. Kase, E. T.; Nikolic, N.; Bakke, S. S.; Bogen, K. K.; Aas, V.; Thoresen, G. H.; Rustan, A. C., Remodeling of oxidative energy metabolism by galactose improves glucose handling and metabolic switching in human skeletal muscle cells. *PloS one* **2013**, 8 (4), e59972.

www.agilent.com/chem/discoverxf

For Research Use Only.
Not for use in diagnostic procedures.

This information is subject to change without notice.

Printed in the USA, June 13, 2019
5994-1057EN

Agilent
Trusted Answers